Supporting Information:

Highly efficient, ultra-stable multi-interlayer luminescent solar concentrators based on green and red-emitting perovskite nanocrystal composites

Changwen Li,[#] Yuxin Gao,[#] Zhiqiang Ren, Shoujun Xiong, Changwei Li, Jun Wu, Jinhua Li, Xianbao Wang,* Jianying Wang**

Key Laboratory for the Green Preparation and Application of Functional Materials, Ministry of Education, Collaborative Innovation Center for Advanced Organic Chemical Materials Co-constructed by the Province and Ministry, Hubei Key Laboratory of Polymer Materials, School of New Energy and Electrical Engineering, Hubei University, Wuhan 430062, P. R. China

* Corresponding authors:

wangjy_2002@hubu.edu.cn (J. Wang)

wujun@hubu.edu.cn (J. Wu)

wxb@hubu.edu.cn (X. Wang)

# These authors contribute to this work equally

Contents

S1 Experimental section

S1.1 Materials

Tetraethyl orthosilicate (TEOS, AR), ammonia solution (NH_3-H_2O, 25-28 wt%), ethanol (EtOH, 99.7%), N-N dimethylamide (DMF, 99.5%), n-hexane (AR), concentrated hydrochloric acid (HCl, 36-38%), and dichloromethane (DCM, 99.5%) were purchased from Sinopharm Chemical Reagent Co. Ltd. Trimethylchlorosilane (TMCS, >98.0%) was purchased from Aladdin Reagent (Shanghai) Co. Lead bromide. ($PbBr_2$, 99.9%), cesium bromide (CsBr, 99.5%), zinc bromide ($ZnBr_2$, 99.9%), and zinc iodide (ZnI_2, 99.9%) were purchased from McLean Co. All basic components and curing agents of polydimethylsiloxane (PDMS Sylgard 184) were obtained from Dow Corning 184 Optical Adhesives, USA. All chemicals were used as is without further purification. All chemicals were used as received, without further purification and modification.

S1.2 Synthesis of silica aerogels

Silicon aerogels were synthesized as improved in previous publications.[1] The molar ratio of alcohol to TEOS was 4:1, the molar ratio of water to TEOS was 2.8, and the

concentration of HCl relative to water was 0.01 mol/L. The mixture was stirred for 8 hours. Under stirring, an ethanol solution of 10% vol. ammonia was added, and the pH was adjusted to 6-7. After aging at room temperature for 24 h, the wet gel showed a light blue color, and n-hexane was added to replace the solvent. TMCS: hexane (3:7 vol%) solution was added, and for complete modification, the molar ratio of TMCS to Si was 4:1, and the modification temperature was 50 ℃ for 5 h. Finally, the gels were dried in an oven, and hydrophobic silica aerogels were obtained after drying at 60, 80, and 120 ℃ for 2 h by gradient temperature increase, respectively. Calcination in air at 500 ℃ for 2 h was used to remove the hydrophobic methyl groups in the silica aerogel structure.

S1.3 Synthesis of Zn-$CsPbBr_3$@SiO_2 (ZB) composites

1 mmol CsBr, x mmol $PbBr_2$, and 1-x mmol $ZnBr_2$ were mixed, followed by adding silica aerogel of the same mass as the template. The mixture was thoroughly ground and blended in a mortar. Subsequently, the homogeneous mixture was transferred to a muffle furnace and calcined at 600 ℃ for 20 min, with a heating rate of 5 ℃/min. After cooling to room temperature, the product was washed three times with deionized water and ethanol. The precipitate was then collected via centrifugation for 5 min and dried in a vacuum oven at 60 ℃. Finally, the ZB composite was obtained through fine grinding of the dried powder. The detailed sample names and precursor quantities are listed in Table S1.

S1.4 Synthesis of Zn-$CsPbBrI_2$@SiO_2 (ZBI) Composites

1 mmol CsBr, 0.5 mmol PbI_2, x mmol $PbBr_2$, and 0.5−x mmol $ZnBr_2$ were mixed, followed by adding silica aerogel of the same mass as the template. The mixture was thoroughly ground and blended in a mortar. The homogeneous mixture was then transferred to a covered porcelain boat and placed in a tube furnace filled with nitrogen gas. It was calcined at 750 ℃ for 30 min at a heating rate of 10 ℃/min. Upon reaching 750 ℃, all gas valves were closed. After natural cooling, the sample was washed several times with DMF and centrifuged. The precipitate was then dried in a vacuum oven at 30 ℃. Finally, the ZBI composite was obtained through fine grinding of the dried powder. Detailed sample names and precursor quantities are listed in Table S2

S1.5 Fabrication of LSCs

Single-interlayer LSCs were prepared as shown in Figure 1. Initially, various masses of ZB/ZBI composites, PDMS curing agent, and DCM were weighed and mixed in a reagent bottle. This mixture was stirred for 30 min and then ultrasonicated for another 30 min to pre-disperse the composite powder in the solution. Subsequently, a specific amount of PDMS host agent was added to the mixture, which was then stirred for 1 hour. During this process, the DCM evaporated, allowing the powder to be completely and uniformly dispersed. The resulting suspension was weighed (100-110 mg) onto a glass substrate (25 × 25 × 1.5 mm^3) using an electronic balance. The mixture was allowed to flow naturally until the mixture fully covered the substrate, after which it was placed under vacuum to eliminate air bubbles. A second glass plate (25 × 25 × 0.3 mm^3) was then placed on top. The laminates were subsequently heat-cured for 1 min on a hot stage at 120 ℃, resulting in single-interlayer LSCs based on ZB/PDMS and

ZBI/PDMS. The thickness of the fluorescent layer was controlled to be 0.2 mm, and the total thickness of the LSCs was approximately 2.0 mm. The detailed dosage of each component are shown in the Table S3.

Preparation of Overall curing LSCs. Generally, a mixture of various masses fractions of ZB/ZBI composite, PDMS, and curing agent (in a mass ratio of 10:1) was prepared. To obtain a homogeneous suspension, the mixture was thoroughly stirred, sonicated, and vacuumed for 1 hour to remove internal air bubbles. The mixtures were then placed in a mold and cured at 60 ℃ for 3 h. The resulting product was the overall cured LSC. The detailed dosage of each component are shown in Supplementary Table S4.

The multi-interlayer LSCs were prepared using the single-interlayer LSCs preparation method. A glass substrate (25 × 25 × 1 mm^3) was chosen as the base layer and drop-coated with 100–110 mg of a ZBI/PDMS mixture (14.0 wt%). This was then covered with another glass plate (25 × 25 × 0.3 mm^3). After thermal curing, a series of ZB/PDMS mixtures (0.5%-14.0 wt%) were drop-coated and covered with additional glass plates (25 × 25 × 0.3 mm^3), followed by thermal curing at 120 ℃ for 1 min. Multi-interlayer LSCs were obtained by controlling the thickness of the fluorescent layer in each layer to 0.2 mm and the total thickness to 2.0 mm.

S2 Characterization

The size and morphology of ZB and ZBI composites were characterized by the high-resolution field-emission transmission electron microscope (HRTEM) on Talos F200X (FEI, Czech). The crystal structure information of the samples was obtained using an X-ray diffraction (XRD) spectrometer on a Bruker D8 phaser with Cu Ka radiation (λ = 1.5406 Å) at angles ranging from 10 to 60°. The elemental analysis was carried out through X-ray photoelectron spectroscopy (XPS) (PHOIBOS150, Germany). The PL excitation and emission spectra of dendritic $CsPbBr_3@SiO_2$ particles were collected via the fluorescent spectrometer (RF-6000, Shimadzu, Japan). The UV-Vis absorption spectra and transmittance spectra were recorded by an ultraviolet-visible-near infrared (UV-vis-NIR) spectrometer (UV-3600 Plus, Shimadzu, Japan). All fluorescence and reflectance spectra were recorded using a fluorescence spectrometer (QE65PRO-FL, Ocean Optics Inc.) and a fiber optic spectrometer (USB4000, Ocean Optics Inc.), respectively. All photographs of LSCs in visible and UV light were taken with a regular camera. The steady-state photoluminescence (PL) and time-resolved photoluminescence (TRPL) (under 375 or 420nm excitation) were obtained by DW-PLE03 (Fluo Time 300). The current density–voltage (*J-V*) curves of the silicon solar cell were measured by a source meter (Keithley 2400, USA) under simulated AM 1.5 G (100 mW/cm^2 irradiance) provided by a solar simulator (Newport Oriel Sol 3A Class AAA, 64023A). Silicon solar cells (Voc: 0.54 V, Jsc: 30 mA/cm^2, PCE: 11% (active area: 0.5 cm^2), EQE: 15% at 510 nm) are purchased from Ningbo Angui Electronics Co., ltd. Most of the surface area of the silicon solar cell was covered by matte black tape, with the exposed area being strictly the same as the edge area of the LSC. The PLQY and edge-emission efficiency (η_{edge}) of all the LSCs were obtained on a fluorescence spectrophotometer (Ocean Optics QE65PRO-FL) with a calibrated integrating sphere.

The external optical efficiency (η_{opt}) can be calculated by using the following equation:

$$\eta_{opt} = \frac{I_{LSC}}{I_{PV} \times G}$$

where I_{LSC} is the short circuit current from a cell attached to the LSC and I_{PV} is the short circuit current measured for the same solar cell under direct illumination with the same light source. G is the ratio of the top surface area (A_{top}) relative to the edge surface area (A_{edge}) of the LSCs.

A majority of the surface area of the silicon solar cell was covered by a black tape and the left surface area of the solar cell is strictly the same as one edge area of the LSCs for measurement of optical efficiency.

η_{int} is defined as the ratio between the number of photons emitted at the edge of the LSC and the number of absorbed incident photons, calculated by the following equation[2]:

$$\eta_{int} = \text{PLQY} \times \eta_{edge}$$

η_{ext} is defined as the ratio between the number of photons emitted at the edge of the LSC and the total number of incident photons, calculated by the following equation[3]:

$$\eta_{ext} = \eta_{int} \times \eta_{abs}$$

where η_{abs} is the absorption factor of LSC at the incident light wavelength, which can be calculated using the following equation:

$$\eta_{abs} = (1 - R) \times (1 - 10^{-OD})$$

R is the reflectance at the incidence light wavelength and OD is the optical density

at the specific wavelength.

The overall power conversion efficiency (η_{PCE}) is calculated by the following equation[4]:

$$\eta_{PCE} = \frac{I_{SC} \times V_{OC} \times FF}{P_{in} \times A_{LSC}}$$

where I_{SC} is the short current, Voc is the open circuit voltage, FF is the fill factor, P_{in} is AM1.5G, A_{LSC} is the LSC top surface.

S3 Figures and tables

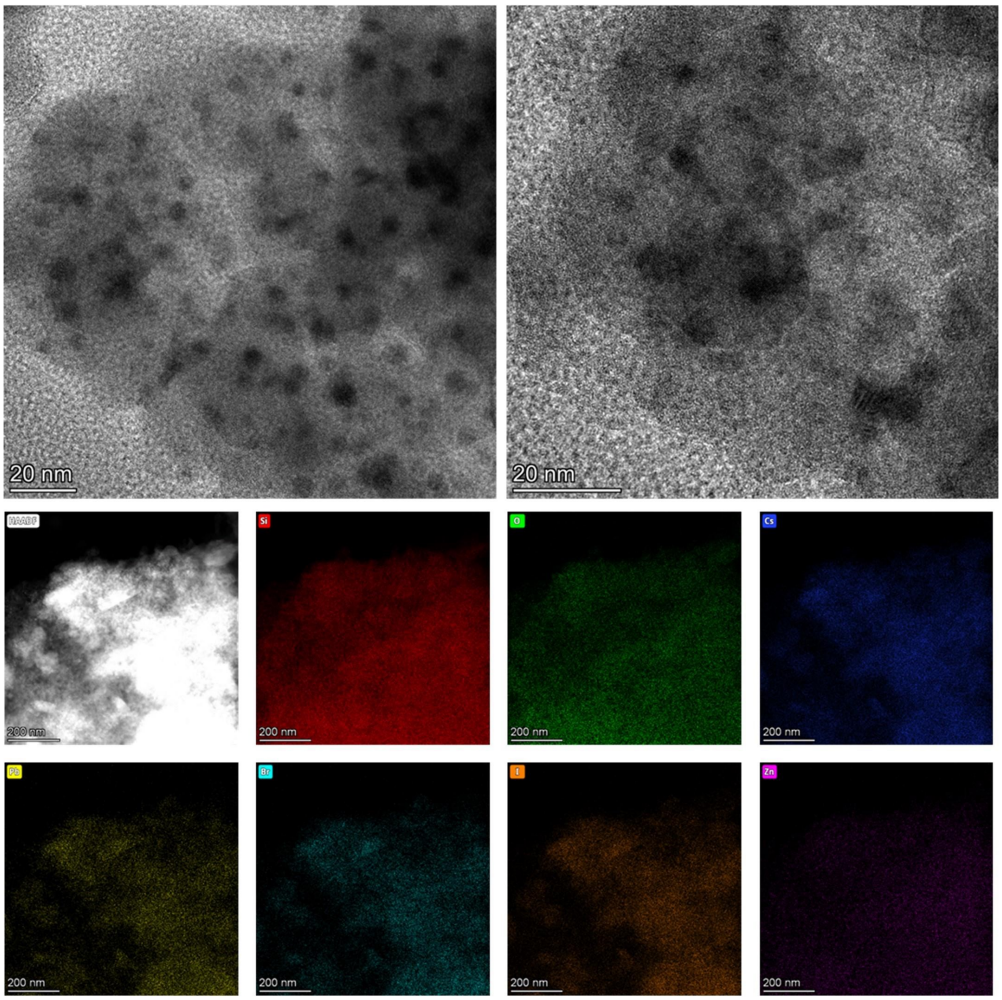

Figure S1. HRTEM image of Zn-$CsPbBrI_2$@SiO_2 composites and HAADF-STEM image of Zn-$CsPbBrI_2$@SiO_2 composites and distribution of Si, O, Cs, Pb, Br, I, Zn elemental mapping in the corresponding region.

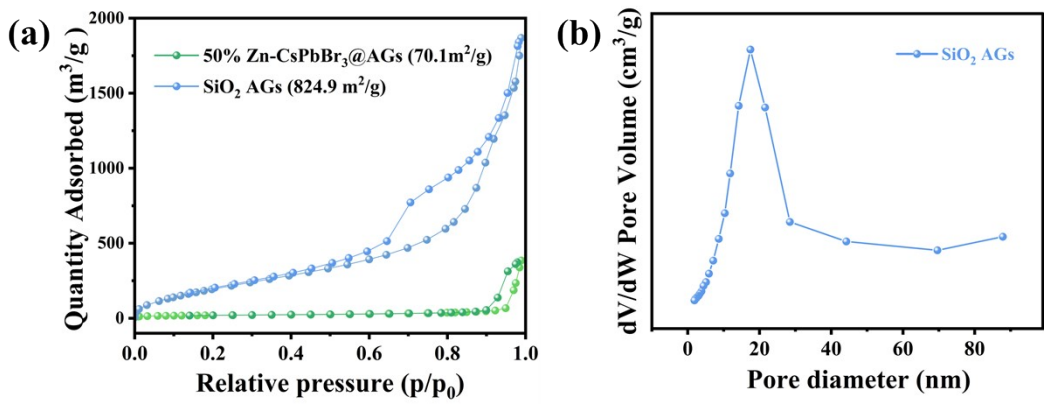

Figure S2. (a) N_2 adsorption−desorption isotherms, (b) the pore size distributions of the AGs.

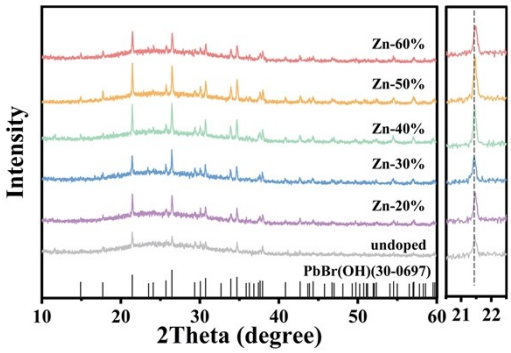

Figure S3. XRD of Zn-$CsPbBr_3$@SiO_2 composites at different Zn^{2+} ion doping concentrations.

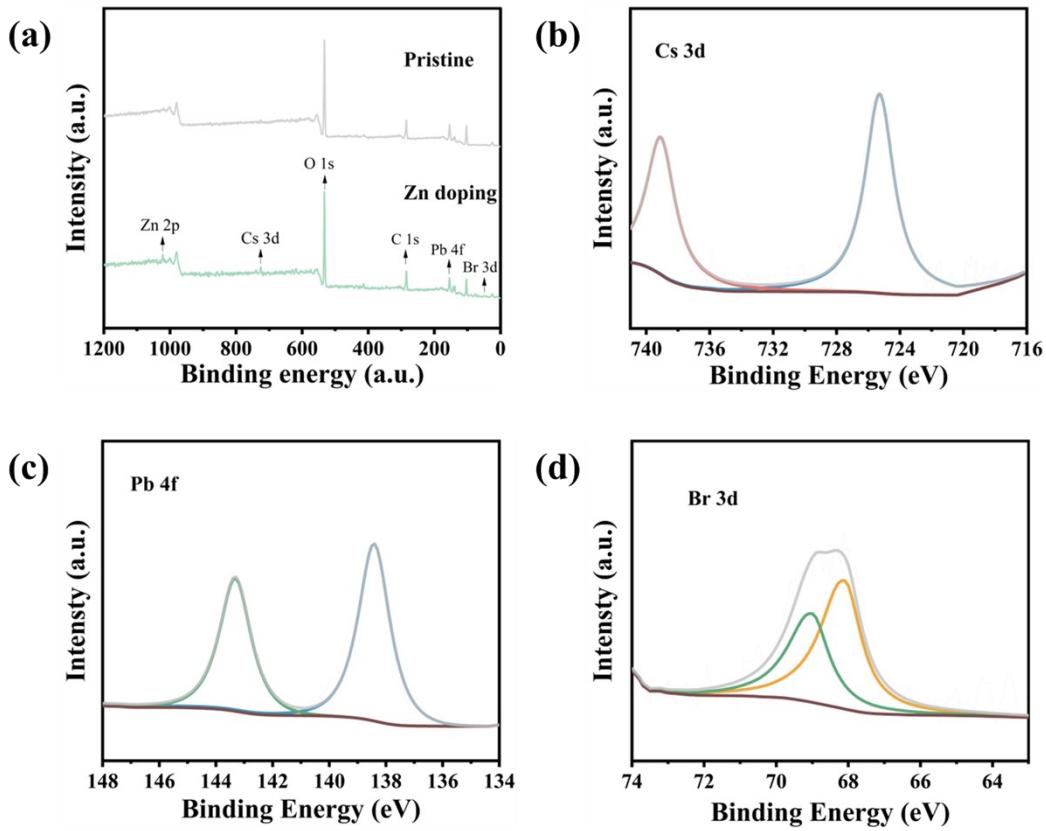

Figure S4. (a) XPS full survey spectrum of the Zn-$CsPbBr_3$@SiO_2 composites. The high-resolution XPS spectra for 50% Zn-$CsPbBr_3$@SiO_2 composites. (b) Cs 3d, (c) Pb 4f, (d) Br 3d.

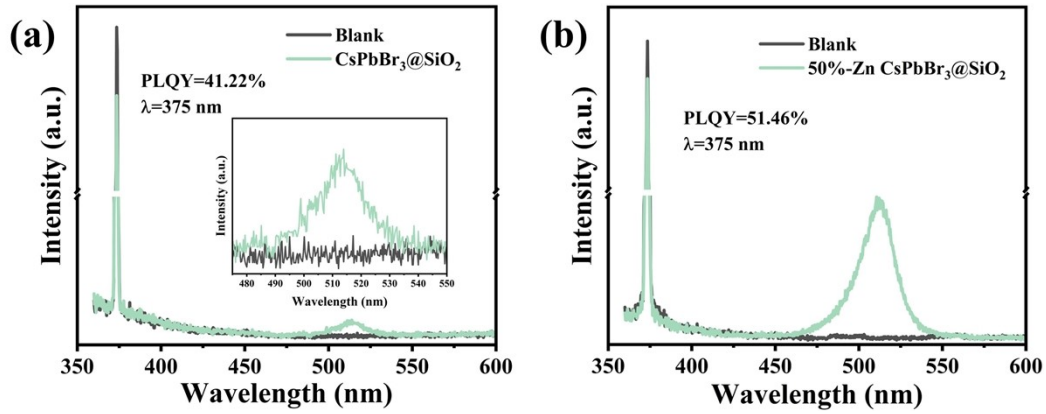

Figure S5. PLQY of undoped (a) and 50% Zn-$CsPbBr_3$@SiO_2 composites (b).

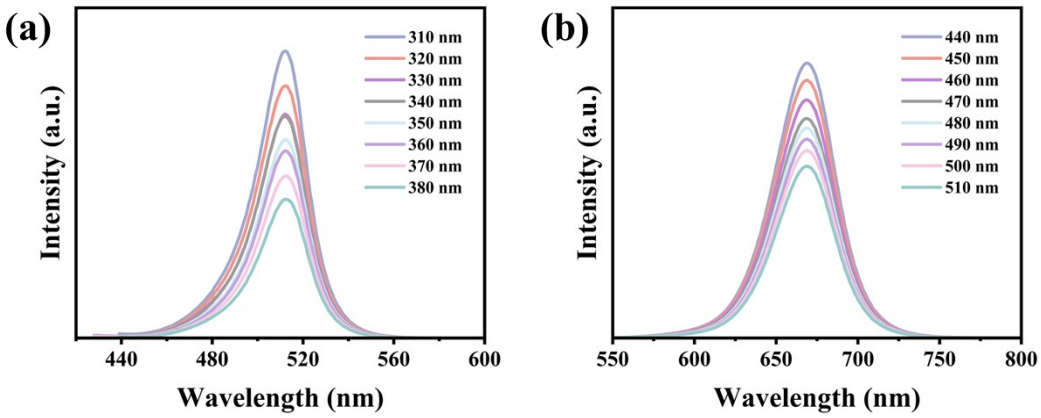

Figure S6. (a) PL spectra of 50% Zn-$CsPbBr_3$@SiO_2 at various excitation wavelengths. (b) PL spectra of 50% Zn-$CsPbBrI_2$@SiO_2 at various excitation wavelengths.

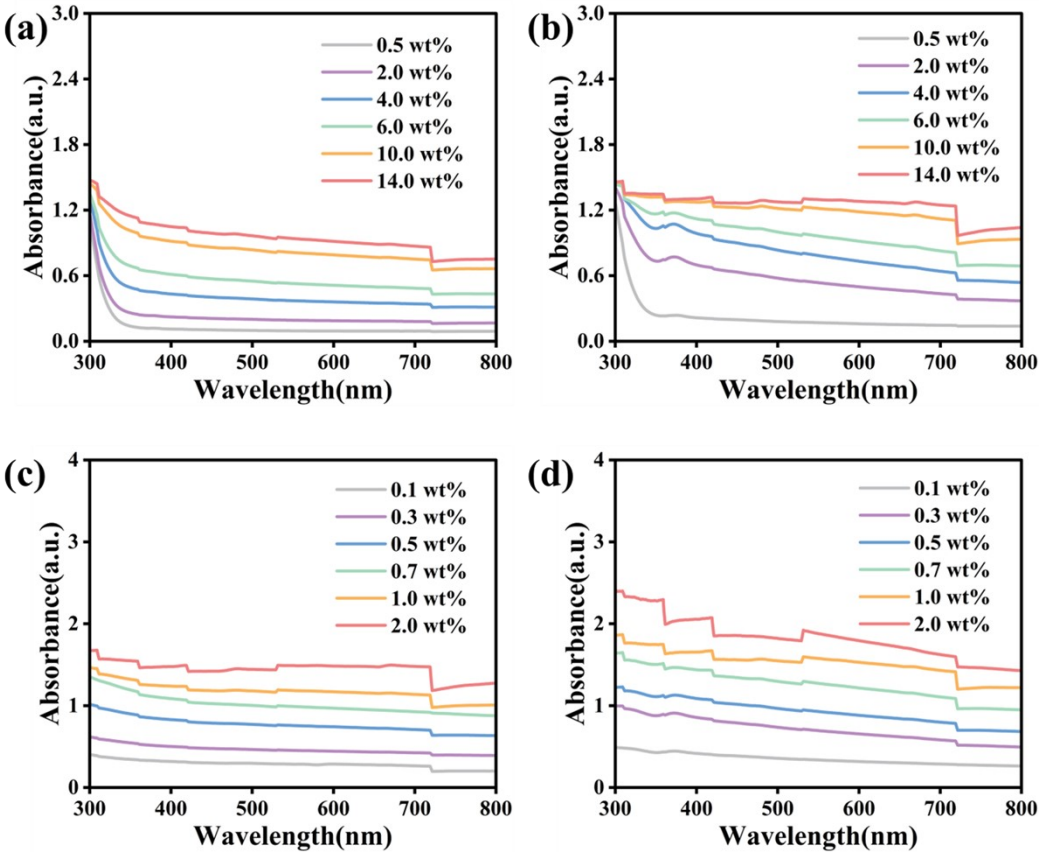

Figure S7. (a-b) Absorption spectra of single-interlayer LSCs with different ZB/ZBI concentrations, respectively. (c-d) PL spectra of overall curing LSCs with different ZB/ZBI concentrations, respectively.

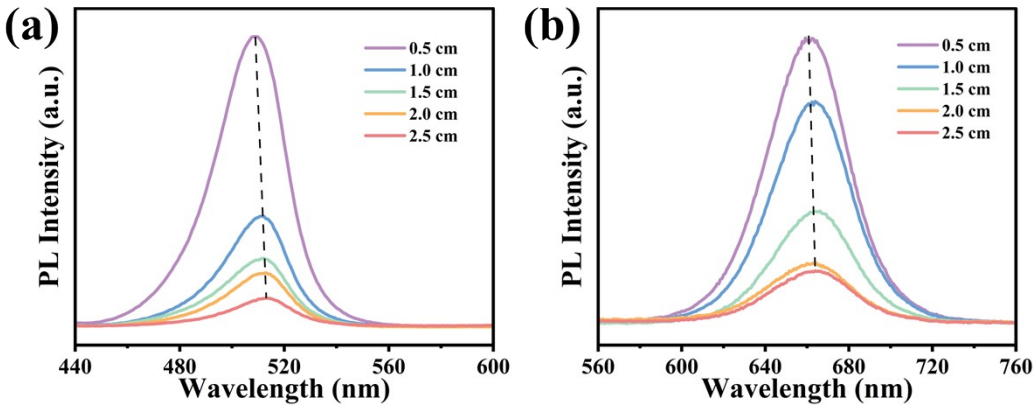

Figure S8. PL spectra of (a) Zn-$CsPbBr_3$@SiO_2 and (b) Zn-$CsPbBrI_2$@SiO_2 of single-interlayer LSCs were measured at different optical intervals (L=0.5, 1.0, 1.5, 2.0 and 2.5 cm).

The distance (L) was defined as the distance between the excitation spot on the LSC and the edge of the LSC.

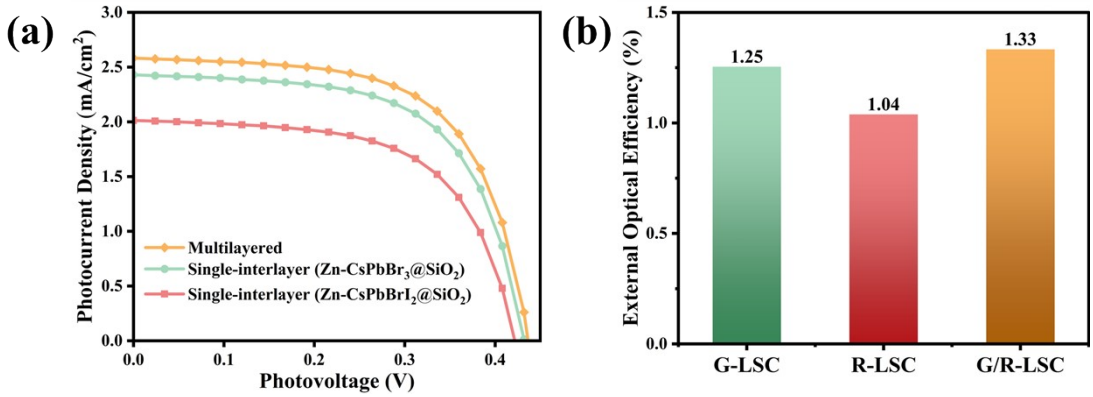

Figure S9. (a) The current density-voltage (*J-V*) curves of large-area single interlayer LSCs and multi-interlayer LSCs (50 × 50 × 2 mm^3) based on ZB/ZBI complexes at a concentration of 4.0 wt%. (b) The corresponding external optical efficiency histograms.

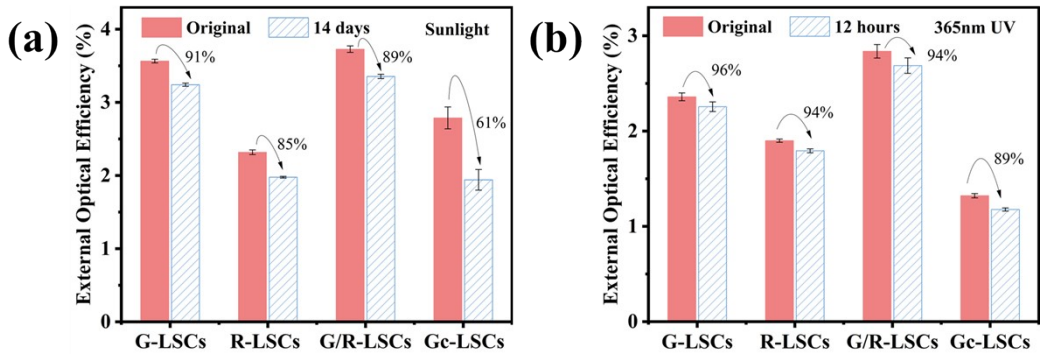

Figure S10. η_{opt} of different types of LSCs before and after 14 days of exposure to (a) natural sunlight and 12 hours of exposure to (b) 365 nm UV light.

Table S1. Molar ratios of proportional precursors at different doping levels for Zn-$CsPbBr_3$@SiO_2 composites.

Mixing ratio	CsBr	$PbBr_2$	$ZnBr_2$
0%	1	1	--
20%	1	0.8	0.2
40%	1	0.6	0.4
50%	1	0.5	0.5
60%	1	0.4	0.6

Table S2. Molar ratios of proportional precursors at different doping levels for Zn-$CsPbBrI_2$@SiO_2 composites.

Mixing ratio	CsI	PbI_2	$PbBr_2$	$ZnBr_2$	ZnI_2
0%	1	0.5	0.5	--	--
20%	1	0.5	0.3	0.2	--
40%	1	0.5	0.1	0.4	--
50%	1	0.5	--	0.5	--
60%	1	--	0.4	0.1	0.5

Table S3. The preparation formula of single-interlayer LSCs.

Content of ZB/ZBI composites	PDMS Sylgard 184 (mg)	curing agent (mg)	ZB/ZBI composite (mg)	DCM (μL)
0.5 wt%	500	50	2.5	250
2.0 wt%	500	50	10	250
4.0 wt%	500	50	20	250
6.0 wt%	500	50	30	250
10.0 wt%	500	50	50	250
14.0 wt%	500	50	70	250

Table S4. The preparation formula of overall-curing LSCs.

Content of ZB/ZBI composites	PDMS Sylgard 184 (mg)	curing agent (mg)	ZB/ZBI composite (mg)	DCM (μL)
0.1 wt%	2500	250	2.5	250
0.3 wt%	2500	250	7.5	250
0.5 wt%	2500	250	12.5	250
0.7 wt%	2500	250	17.5	250
1.0 wt%	2500	250	25	250
2.0 wt%	2500	250	50	250

Table S5. Lifetime data of Zn-$CsPbBr_3$@SiO_2 composite (under 375 nm excitation) and Zn-$CsPbBrI_2$@SiO_2 composite (under 420 nm excitation).

	λ_{ex} (nm)	A_1	τ_1 (ns)	A_2	τ_2 (ns)	A_3	T_3 (ns)	τ_{avg} (ns)	χ^2
$CsPbBr_3$@SiO_2	375.00	0.32	25.63	0.65	6.75	0.06	132.39	62.40	0.999
50%Zn-$CsPbBr_3$@SiO_2	375.00	1.01	5.21	0.58	14.19	0.07	60.02	75.55	0.999
$CsPbBrI_2$@SiO_2	420.00	1.25	3.87	0.45	23.38	0.09	147.17	22.32	0.998
50%Zn-$CsPbBrI_2$@SiO_2	420.00	0.77	4.97	0.59	19.02	0.14	63.14	33.15	0.999

Table S6. Photovoltaic parameters of single-interlayer LSCs with different concentrations of ZB composites.

	$J_{sc}(mA/cm^2)$	$V_{oc}(V)$	$FF(\%)$	G	$\eta_{opt}(\%)$	C	$\eta_{PCE}(\%)$
0.5 wt%	1.52	0.43	59.74	3.125	1.567	0.05	0.126
2.0 wt%	2.25	0.45	63.01	3.125	2.326	0.07	0.204
4.0 wt%	2.93	0.46	64.85	3.125	3.029	0.09	0.281
6.0 wt%	3.36	0.47	65.78	3.125	3.465	0.11	0.329
10.0 wt%	3.87	0.47	65.93	3.125	3.997	0.12	0.382
14.0 wt%	4.22	0.47	66.23	3.125	4.357	0.14	0.423

Table S7. Photovoltaic parameters of single-interlayer LSCs with different concentrations of ZBI composite.

	$J_{sc}(mA/cm^2)$	$V_{oc}(V)$	$FF(\%)$	G	$\eta_{opt}(\%)$	C	$\eta_{PCE}(\%)$
0.5 wt%	1.31	0.42	57.98	3.125	1.353	0.04	0.101
2.0 wt%	1.99	0.44	61.57	3.125	2.054	0.06	0.172
4.0 wt%	2.26	0.45	62.44	3.125	2.336	0.07	0.202
6.0 wt%	2.60	0.46	63.64	3.125	2.682	0.08	0.241
10.0 wt%	3.10	0.46	64.72	3.125	3.204	0.10	0.297
14.0 wt%	3.49	0.47	65.97	3.125	3.605	0.11	0.346

Table S8. Photovoltaic parameters of overall curing LSCs with different concentrations of ZBI composite.

	$J_{sc}(mA/cm^2)$	$V_{oc}(V)$	$FF(\%)$	G	$\eta_{opt}(\%)$	C	$\eta_{PCE}(\%)$
0.1 wt%	4.03	0.46	65.49	3.125	4.162	0.13	0.387
0.3 wt%	5.43	0.47	66.89	3.125	5.605	0.18	0.546
0.5 wt%	6.79	0.48	68.10	3.125	7.005	0.22	0.707
0.7 wt%	7.23	0.48	68.41	3.125	7.463	0.23	0.761
1.0 wt%	8.22	0.49	69.59	3.125	8.488	0.27	0.890
2.0 wt%	9.01	0.49	69.50	3.125	9.298	0.29	0.980

Table S9. Photovoltaic parameters of overall curing LSCs with different concentrations of ZBI composite.

	$J_{sc}(mA/cm^2)$	$V_{oc}(V)$	$FF(\%)$	G	$\eta_{opt}(\%)$	C	$\eta_{PCE}(\%)$
0.1 wt%	2.49	0.44	63.11	3.125	2.574	0.08	0.220
0.3 wt%	3.43	0.45	65.18	3.125	3.541	0.11	0.323
0.5 wt%	4.04	0.46	65.69	3.125	4.165	0.13	0.389
0.7 wt%	4.68	0.46	66.58	3.125	4.826	0.15	0.462
1.0 wt%	5.14	0.47	67.34	3.125	5.310	0.17	0.519
2.0 wt%	5.79	0.47	67.14	3.125	5.972	0.19	0.585

Table S10. The optical efficiency of single-interlayer LSCs with different concentrations of ZB composite.

	PLQY(%)	η_{edge}**(%)**	η_{int}**(%)**	η_{abs}**(%)**	η_{ext}**(%)**
0.5 wt%	49.31%	44.03%	21.71%	20.79%	4.51%
2.0 wt%	61.88%	53.00%	32.80%	38.84%	12.74%
4.0 wt%	78.96%	44.01%	34.75%	57.81%	20.09%
6.0 wt%	80.50%	34.67%	27.91%	74.15%	20.70%
10.0 wt%	84.13%	27.10%	22.80%	83.82%	19.11%
14.0 wt%	92.70%	24.81%	23.00%	87.79%	20.19%

Table S11. The optical efficiency of single-interlayer LSCs with different concentrations of ZBI composite.

	PLQY(%)	η_{edge}(%)	η_{int}(%)	η_{abs}(%)	η_{ext}(%)
0.5 wt%	50.68%	42.30%	21.44%	36.59%	7.85%
2.0 wt%	48.96%	30.61%	14.99%	78.60%	11.78%
4.0 wt%	44.94%	26.20%	11.77%	91.58%	10.78%
6.0 wt%	46.05%	18.59%	8.56%	93.21%	7.98%
10.0 wt%	33.90%	14.23%	4.82%	94.98%	4.58%
14.0 wt%	33.30%	12.61%	4.20%	94.56%	3.97%

Table S12. The optical efficiency of overall curing LSCs with different concentrations of ZB composite.

	PLQY(%)	η_{edge}(%)	η_{int}(%)	η_{abs}(%)	η_{ext}(%)
0.1 wt%	52.68%	56.89%	29.97%	20.79%	6.23%
0.3 wt%	61.49%	52.16%	32.07%	38.84%	12.46%
0.5 wt%	83.63%	39.97%	33.43%	57.81%	19.33%
0.7 wt%	70.80%	35.74%	25.31%	74.15%	18.77%
1.0 wt%	73.48%	29.25%	21.49%	83.82%	18.02%
2.0 wt%	76.54%	26.20%	20.05%	87.79%	17.60%

Table S13. The optical efficiency of overall curing LSCs with different concentrations of ZBI composite.

	PLQY(%)	η_{edge}(%)	η_{int}(%)	η_{abs}(%)	η_{ext}(%)
0.1 wt%	35.68%	39.37%	14.05%	62.95%	8.84%
0.3 wt%	24.87%	35.64%	8.86%	86.15%	7.63%
0.5 wt%	24.44%	29.94%	7.32%	90.86%	6.65%
0.7 wt%	21.25%	25.55%	5.43%	92.81%	5.04%
1.0 wt%	20.63%	26.45%	5.46%	93.05%	5.08%
2.0 wt%	15.83%	12.21%	1.93%	93.45%	1.81%

Table S14. The η_{opt} for LSCs with different luminophores, waveguides, and dimensions.

Luminophore	Waveguide	Dimensions (cm^3)	η_{opt} (%)	Ref.
$CsPbBr_3$ QDs	EVA	2.5 × 2.5 × 0.2	1.66	5
$CsPbI_3$ QDs	EVA	2.5 × 2.5 × 0.2	2.14	5
$CsPb(Br_xI_{1-x})_3$	PLMA-EGDA	9 × 1.3 × 0.2	2	6
Cs_4PbBr_6 NCs	PS	10 × 10 × 0.4	2.4	7
$CsPb(Br_{0.2}I_{0.8})_3$ NCs	PLMA-EGDA	10 × 10 × 0.2	2.4	8
Yb^{3+}-doped $CsPbCl_3$	PMMA	5 × 5 × 0.2	3.7	9
Mn^{2+}-$CsPbCl_3$ NCs	PMMA	20 × 20 × 0.5	0.9	10
$CsPbBr_3$ NCs	Glass	2 × 2 × 0.11	6.17	11
$CsPbX_3$ (laminated)	PLMA/PMMA	5 × 5 × 0.7	4.97	12
Zn-$CsPbBr_3$@SiO_2	PDMS	2.5 × 2.5 × 0.2	4.36	This work
Zn-$CsPbBrI_2$@SiO_2	PDMS	2.5 × 2.5 × 0.2	3.61	This work
$CsPbX_3$@SiO_2 (tandem)	PDMS	2.5 × 2.5 × 0.2	4.72	This work
Zn-$CsPbBr_3$@SiO_2 (overall curing)	PDMS	2.5 × 2.5 × 0.2	9.38	This work
Zn-$CsPbBrI_2$@SiO_2 (overall curing)	PDMS	2.5 × 2.5 × 0.2	5.97	This work

Reference

1 Y. Du, X. Zhang, J. Wang, Z. Liu, K. Zhang, X. Ji, Y. You and X. Zhang, *ACS Nano*, 2020, **14**, 11919–11928.

2 M. G. Debije, R. C. Evans and G. Griffini, *Energy Environ Sci*, 2021, **14**, 293–301.

3 T. Wei, L. Wang, C. Sun, D. Xu, J. Tao, H. Zhang, J. Han, C. Fan, Z. Zhang and W. Bi, *ACS Appl. Mater. Interfaces*, 2021, **13**, 56348–56357.

4 S. Castelletto and A. Boretti, *Nano Energy*, 2023, **109**, 108269.

5 C. Cai, M. Wang, J. Wang, B. Xu, J. Wang, L. Zhang, W. Xin, L. Xue, J. Li and X. Wang, *Appl. Surf. Sci.*, 2023, **609**, 155313.

6 H. Zhao, Y. Zhou, D. Benetti, D. Ma and F. Rosei, *Nano Energy*, 2017, **37**, 214–223.

7 H. Zhao, R. Sun, Z. Wang, K. Fu, X. Hu and Y. Zhang, *Adv. Funct. Mater.*, 2019, **29**, 1902262.

8 H. Zhao, D. Benetti, X. Tong, H. Zhang, Y. Zhou, G. Liu, D. Ma, S. Sun, Z. M. Wang, Y. Wang and F. Rosei, *Nano Energy*, 2018, **50**, 756–765.

9 X. Zuo, K. Chang, J. Zhao, Z. Xie, H. Tang, B. Li and Z. Chang, *J. Mater. Chem.A*, 2016, **4**, 51–58.

10 F. Meinardi, Q. A. Akkerman, F. Bruni, S. Park, M. Mauri, Z. Dang, L. Manna and S. Brovelli, *ACS Energy Lett.*, 2017, **2**, 2368–2377.

11 Y. Zhang, W. Zhang, Y. Ye, K. Li, X. Gong and C. Liu, *Sol. Energy Mater. Sol. Cells*, 2022, **238**, 111619.

12 X. Liu, D. Benetti, J. Liu, L. Jin and F. Rosei, *Nano Energy*, 2023, **111**, 108438.